

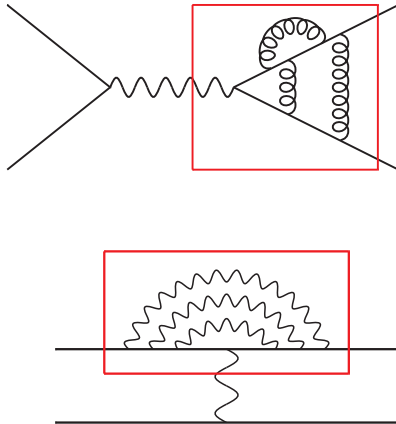
# Towards $N^3\text{LO}$ : three-loop form factors

5th Workstop / Thinkstart: Radiative corrections and Monte Carlo tools for Strong 2020 | June 5 - 9, 2023

Fabian Lange

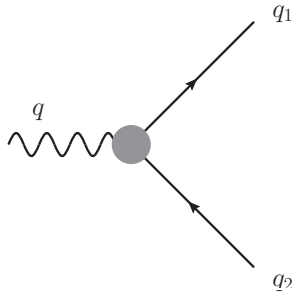
in collaboration with Matteo Fael, Kay Schönwald, Matthias Steinhauser | June 6, 2023

# Motivation



- Form factors are basic building blocks for many physical observables:
  - $t\bar{t}$  production at hadron and  $e^+e^-$  colliders
  - Higgs production and decay
  - Low-energy  $e^+e^-$  collisions and  $\mu e$  scattering
  - ...
- Form factors exhibit an universal infrared behavior which is interesting to study

# The process

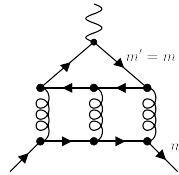
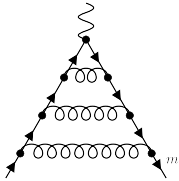


$$X(q) \rightarrow Q(q_1) + \bar{Q}(q_2)$$

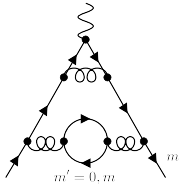
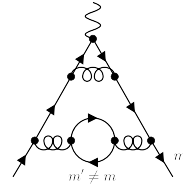
$$q_1^2 = q_2^2 = m^2, \quad q^2 = s = \hat{s} \cdot m^2$$

vector :	$j_\mu^\nu = \bar{\psi} \gamma_\mu \psi,$	$\Gamma_\mu^\nu = F_1^\nu(s) \gamma_\mu - \frac{i}{2m} F_2^\nu(s) \sigma_{\mu\nu} q^\nu$
axial-vector :	$j_\mu^a = \bar{\psi} \gamma_\mu \gamma_5 \psi,$	$\Gamma_\mu^a = F_1^a(s) \gamma_\mu \gamma_5 - \frac{1}{2m} F_2^a(s) q_\mu \gamma_5$
scalar :	$j^s = m \bar{\psi} \psi,$	$\Gamma^s = m F^s(s)$
pseudo-scalar :	$j^p = im \bar{\psi} \gamma_5 \psi,$	$\Gamma^p = im F^p(s) \gamma_5$

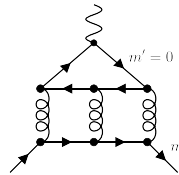
# Types of contributions



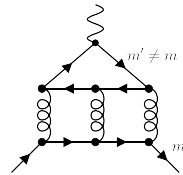
$n_h$  singlet



nonsinglet



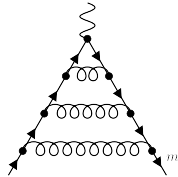
$n_l$  singlet



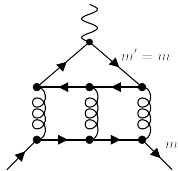
contributions with  $m' \neq m$

# Status of massive QCD corrections

nonsinglet:



singlet:



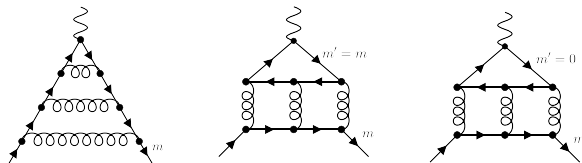
$F_i^{(2)}$  (NNLO):

- fermionic contributions [Hoang, Teubner 1997]
- QED [Bonciani, Mastrolia, Remiddi 2003]
- complete (except contributions with  $m' \neq m$ ) [Bernreuther, Bonciani, Gehrmann, Heinesch, Leineweber, Mastrolia, Remiddi 2004 - 2005]

$F_i^{(3)}$  (NNNLO):

- nonsinglet large  $N_c$  [Henn, Smirnov, Smirnov, Steinhauser 2016; Lee, Smirnov, Smirnov, Steinhauser 2018; Ablinger, Blümlein, Marquard, Rana, Schneider 2 × 2018; Lee, Smirnov, Smirnov, Steinhauser 2018]
- nonsinglet  $n_l$  [Lee, Smirnov, Smirnov, Steinhauser 2018; Ablinger, Blümlein, Marquard, Rana, Schneider 2 × 2018]
- nonsinglet  $n_h$  (partially) [Blümlein, Marquard, Rana, Schneider 2019]
- complete (except contributions with  $m' \neq m$ ) [Fael, FL, Schönwald, Steinhauser 2 × 2022 + 2023]

# Setup



	nonsinglet	$n_h$ -singlet	$n_l$ -singlet
diagrams	271	66	66
families	34	17	13
integrals	302671	106883	127980
masters	422	316	158

- Generate diagrams with `qgraf` [Nogueira 1991]
- Map to predefined integral families with `q2e/exp` [Harlander, Seidensticker, Steinhauser 1998; Seidensticker 1999]
- FORM [Vermaseren 2000; Kuipers, Ueda, Vermaseren, Vollinga 2013; Ruijl, Ueda, Vermaseren 2017] for Lorentz, Dirac, and color algebra [van Ritbergen, Schellekens, Vermaseren 1998]
- Reduction to master integrals with `Kira` [Maierhöfer, Usovitsch, Uwer 2017; Klappert, FL, Maierhöfer, Usovitsch 2020] and `Fermat` [Lewis]
  - Construct good basis where denominators factorize in  $\epsilon$  and  $\hat{s}$  with `ImproveMasters.m` [Smirnov, Smirnov 2020]
- Establish differential equations in  $\hat{s}$  with `LiteRed` [Lee 2012 + 2013]

# Algorithm to solve master integrals (I)

$$\frac{\partial}{\partial \hat{s}} M_n = A_{nm}(\epsilon, \hat{s}) M_m$$

- Compute expansion around  $\hat{s} = 0$  by:
  - Inserting an ansatz for the master integrals into the differential equation:

$$M_n(\epsilon, \hat{s} = 0) = \sum_{i=-3}^{\infty} \sum_{j=0}^{j_{\max}} c_{ij}^{(n)} \epsilon^i \hat{s}^j$$

- Compare coefficients in  $\epsilon$  and  $\hat{s}$  to establish linear system of equations for  $c_{ij}^{(n)}$ :

$$c_{12}^{(1)} \epsilon \hat{s}^2 + \dots = 52 c_{33}^{(1)} \epsilon \hat{s}^2 + \dots + 127 c_{14}^{(4)} \epsilon \hat{s}^2 + \dots$$

- Solve system in terms of small number of boundary constants using Kira with FireFly [Klappert, FL 2019; Klappert, Klein, FL 2020] :

$$c_{12}^{(1)} = 52 c_{33}^{(1)} + 127 c_{14}^{(4)}$$

- Compute boundary values to fix remaining constants

## Algorithm to solve master integrals (II)

$$\frac{\partial}{\partial \hat{s}} M_n = A_{nm}(\epsilon, \hat{s}) M_m$$

- Repeat for  $\hat{s} = \hat{s}_1$ :
  - Insert an ansatz around  $\hat{s} = \hat{s}_1$  into the differential equation:

$$M_n(\epsilon, \hat{s} = \hat{s}_1) = \sum_{i=-3}^{\infty} \sum_{j=0}^{j_{\max}} c_{ij}^{(n)} \epsilon^i (\hat{s} - \hat{s}_1)^j$$

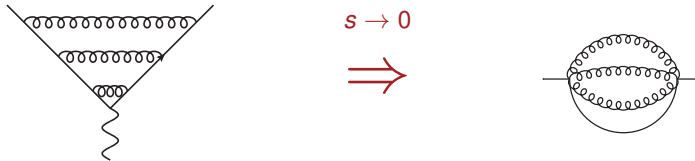
- Compare coefficients in  $\epsilon$  and  $\hat{s}$  and solve system:

$$c_{12}^{(1)} \epsilon (\hat{s} - \hat{s}_1)^2 + \dots = 12c_{44}^{(1)} \epsilon (\hat{s} - \hat{s}_1)^2 + \dots - 23c_{04}^{(4)} \epsilon (\hat{s} - \hat{s}_1)^2 + \dots \quad \Rightarrow \quad c_{12}^{(1)} = 12c_{44}^{(1)} - 23c_{04}^{(4)}$$

- Match this new expansion to previous expansion around  $\hat{s} = 0$  numerically in between, e.g. at  $\hat{s}_1/2$ , to fix the boundary constants
  - Repeat

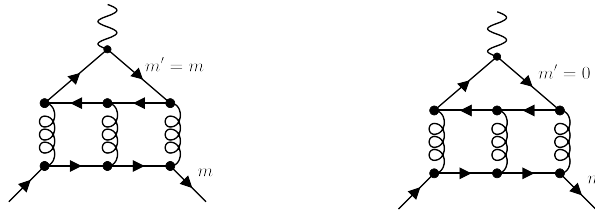


# Calculation of boundary conditions: nonsinglet



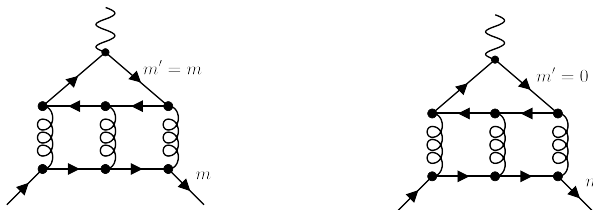
- For  $s = 0$  the nonsinglet master integrals reduce to 3-loop on-shell propagators:
  - Well studied in the literature [Laporta, Remiddi 1996; Melnikov, van Ritbergen 1999; Lee, Smirnov 2010]
  - Some higher-order terms were missing for our calculation
  - Using the dimensional-recurrence relations from [Lee, Smirnov 2010] we calculated them with `SummerTime.m` [Lee, Mingulov 2015] and `PSLQ` [Ferguson, Bailey, Arno 1999]

# Calculation of boundary conditions: singlet



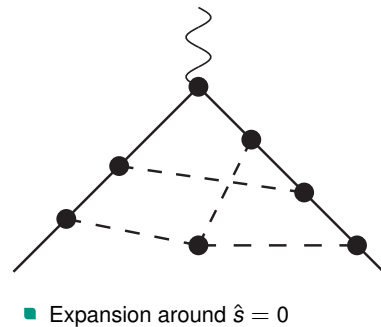
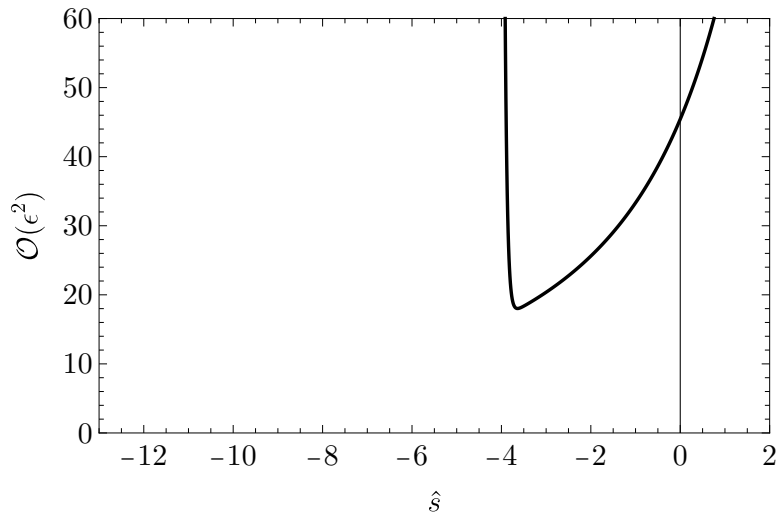
- $n_h$  singlet boundary conditions require asymptotic expansion due to massless cuts:
  - Reveal regions with ASY . m [Smirnov, Pak 2010; Jantzen, Smirnov, Smirnov 2012]
  - Naive region same as for nonsinglet
  - Remaining regions can be integrated directly or with HyperInt [Panzer 2014]

# Calculation of boundary conditions: singlet

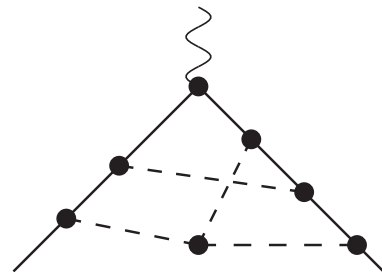
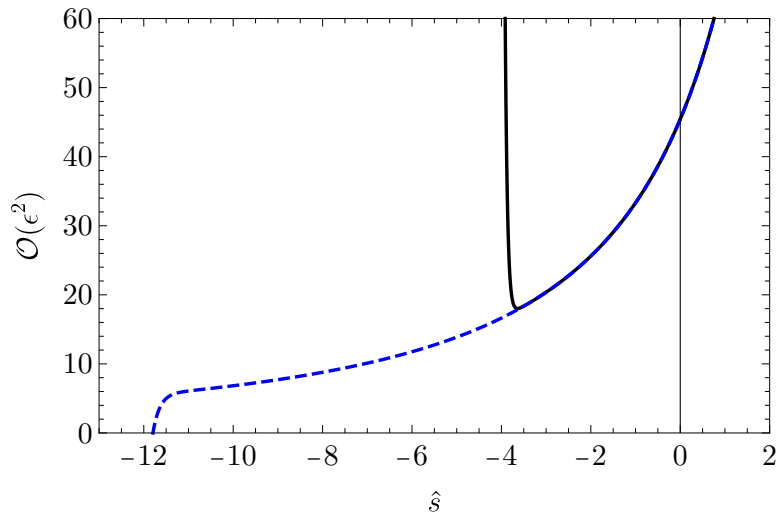


- $n_h$  singlet boundary conditions require asymptotic expansion due to massless cuts:
  - Reveal regions with ASY.m [Smirnov, Pak 2010; Jantzen, Smirnov, Smirnov 2012]
  - Naive region same as for nonsinglet
  - Remaining regions can be integrated directly or with HyperInt [Panzer 2014]
- $n_l$  singlet boundary conditions:
  - Even more massless cuts and direct integration for some regions too complicated
  - Instead use AMFlow [Liu, Ma 2022] to compute them numerically at  $\hat{s} = -1$  with 86 digits

# Example

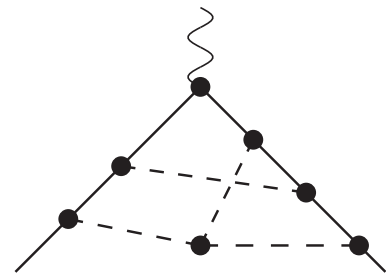
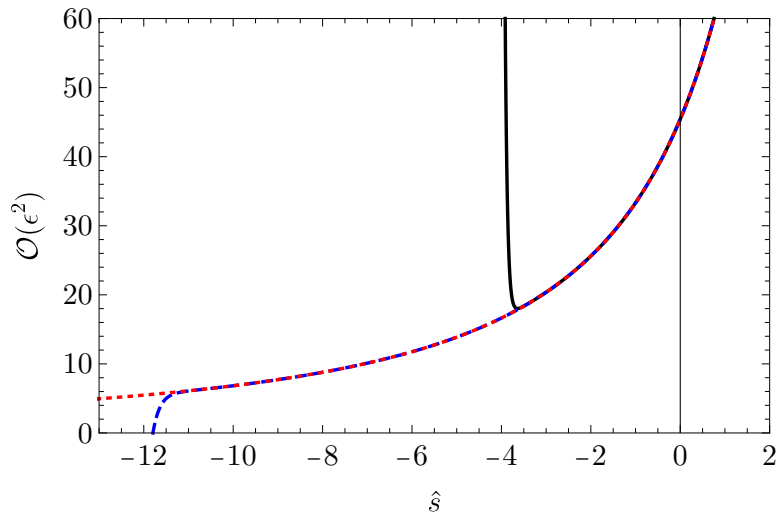


# Example



- Expansion around  $\hat{\delta} = 0$
- Expansion around  $\hat{\delta} = -4$ ,  
matched at  $\hat{\delta} = -2$

# Example



- Expansion around  $\hat{s} = 0$
- Expansion around  $\hat{s} = -4$ ,  
matched at  $\hat{s} = -2$
- Expansion around  $\hat{s} = -8$ ,  
matched at  $\hat{s} = -6$

# Results – analytic expansion around $\hat{s} = 0$

$$\begin{aligned}
 F_1^{v,f,(3)}(\hat{s} = 0) = & \left\{ C_F^3 \left( -15a_4 - \frac{17\pi^2\zeta_3}{24} - \frac{18367\zeta_3}{1728} + \frac{25\zeta_5}{8} - \frac{5l_2^4}{8} - \frac{19}{40}\pi^2 l_2^2 + \frac{4957\pi^2 l_2}{720} + \frac{3037\pi^4}{25920} \right. \right. \\
 & - \frac{24463\pi^2}{7776} + \frac{13135}{20736} \Big) + C_A C_F^2 \left( \frac{19a_4}{2} - \frac{\pi^2\zeta_3}{9} + \frac{17725\zeta_3}{3456} - \frac{55\zeta_5}{32} + \frac{19l_2^4}{48} - \frac{97}{720}\pi^2 l_2^2 \right. \\
 & + \frac{29\pi^2 l_2}{240} - \frac{347\pi^4}{17280} - \frac{4829\pi^2}{10368} + \frac{707}{288} \Big) + C_A^2 C_F \left( -a_4 + \frac{7\pi^2\zeta_3}{96} + \frac{4045\zeta_3}{5184} - \frac{5\zeta_5}{64} - \frac{l_2^4}{24} \right. \\
 & \left. \left. + \frac{67}{360}\pi^2 l_2^2 - \frac{5131\pi^2 l_2}{2880} + \frac{67\pi^4}{8640} + \frac{172285\pi^2}{186624} - \frac{7876}{2187} \right) \right\} \hat{s} + \text{fermionic corrections} + \mathcal{O}(\hat{s}^2)
 \end{aligned}$$

- $l_2 = \ln(2)$ ,  $a_4 = \text{Li}_4(1/2)$  and  $C_A = 3$ ,  $C_F = 4/3$  for QCD
- Expansions for all currents are available up to  $\mathcal{O}(\hat{s}^{67})$

# Results – high-energy limit

$$\begin{aligned}
 F_1^{v,f,(3)} \Big|_{s \rightarrow -\infty} &= 4.7318 C_F^3 - 20.762 C_F^2 C_A + 8.3501 C_F C_A^2 + \left[ 3.4586 C_F^3 - 4.0082 C_F^2 C_A - 6.3561 C_F C_A^2 \right] l_s \\
 &+ \left[ 1.4025 C_F^3 + 0.51078 C_F^2 C_A - 2.2488 C_F C_A^2 \right] l_s^2 + \left[ 0.062184 C_F^3 + 0.90267 C_F^2 C_A - 0.42778 C_F C_A^2 \right] l_s^3 \\
 &+ \left[ -0.075860 C_F^3 + 0.20814 C_F^2 C_A - 0.035011 C_F C_A^2 \right] l_s^4 + \left[ -0.023438 C_F^3 + 0.019097 C_F^2 C_A \right] l_s^5 \\
 &+ \left[ -0.0026042 C_F^3 \right] l_s^6 - \left\{ -92.918 C_F^3 + 123.65 C_F^2 C_A - 47.821 C_F C_A^2 + \left[ -10.381 C_F^3 + 2.3223 C_F^2 C_A \right. \right. \\
 &+ \left. \left. 17.305 C_F C_A^2 \right] l_s + \left[ 4.9856 C_F^3 - 19.097 C_F^2 C_A + 8.0183 C_F C_A^2 \right] l_s^2 + \left[ 3.0499 C_F^3 - 6.8519 C_F^2 C_A + 1.9149 C_F C_A^2 \right] l_s^3 \right. \\
 &+ \left[ 0.67172 C_F^3 - 0.91213 C_F^2 C_A + 0.24069 C_F C_A^2 \right] l_s^4 + \left[ 0.13229 C_F^3 - 0.051389 C_F^2 C_A + 0.0043403 C_F C_A^2 \right] l_s^5 \\
 &+ \left. \left[ 0.0041667 C_F^3 - 0.0010417 C_F^2 C_A - 0.00052083 C_F C_A^2 \right] l_s^6 \right\} \frac{m^2}{s} + \mathcal{O} \left( \frac{m^4}{s^2} \right) + \text{fermionic contributions}
 \end{aligned}$$



# Results – high-energy limit

$$\begin{aligned}
 F_1^{v,f,(3)} \Big|_{s \rightarrow -\infty} &= 4.7318 C_F^3 - 20.762 C_F^2 C_A + 8.3501 C_F C_A^2 + \left[ 3.4586 C_F^3 - 4.0082 C_F^2 C_A - 6.3561 C_F C_A^2 \right] l_s \\
 &+ \left[ 1.4025 C_F^3 + 0.51078 C_F^2 C_A - 2.2488 C_F C_A^2 \right] l_s^2 + \left[ 0.062184 C_F^3 + 0.90267 C_F^2 C_A - 0.42778 C_F C_A^2 \right] l_s^3 \\
 &+ \left[ -0.075860 C_F^3 + 0.20814 C_F^2 C_A - 0.035011 C_F C_A^2 \right] l_s^4 + \left[ -0.023438 C_F^3 + 0.019097 C_F^2 C_A \right] l_s^5 \\
 &+ \left[ -0.0026042 C_F^3 \right] l_s^6 - \left\{ -92.918 C_F^3 + 123.65 C_F^2 C_A - 47.821 C_F C_A^2 + \left[ -10.381 C_F^3 + 2.3223 C_F^2 C_A \right. \right. \\
 &+ 17.305 C_F C_A^2 \Big] l_s + \left[ 4.9856 C_F^3 - 19.097 C_F^2 C_A + 8.0183 C_F C_A^2 \right] l_s^2 + \left[ 3.0499 C_F^3 - 6.8519 C_F^2 C_A + 1.9149 C_F C_A^2 \right] l_s^3 \\
 &+ \left[ 0.67172 C_F^3 - 0.91213 C_F^2 C_A + 0.24069 C_F C_A^2 \right] l_s^4 + \left[ 0.13229 C_F^3 - 0.051389 C_F^2 C_A + 0.0043403 C_F C_A^2 \right] l_s^5 \\
 &+ \left. \left[ 0.0041667 C_F^3 - 0.0010417 C_F^2 C_A - 0.00052083 C_F C_A^2 \right] l_s^6 \right\} \frac{m^2}{s} + \mathcal{O} \left( \frac{m^4}{s^2} \right) + \text{fermionic contributions}
 \end{aligned}$$

- Dedicated calculation of leading logarithms [Liu, Penin, Zerf 2017]:

$$F_1^{v,f,(3)} = -\frac{C_F^3}{384} l_s^6 - \frac{m^2}{s} \left( \frac{C_F^3}{240} - \frac{C_F^2 C_A}{960} - \frac{C_F C_A^2}{1920} \right) l_s^6 + \dots, \quad \text{with } l_s = \ln \left( \frac{m^2}{-s} \right)$$

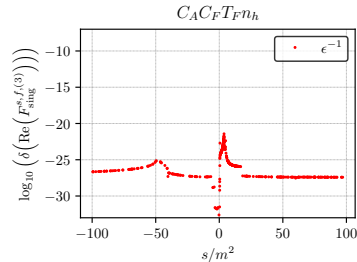
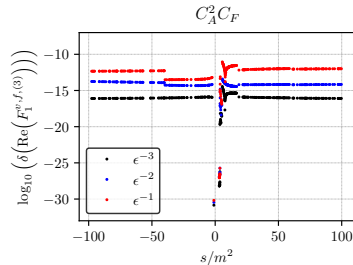
- We reproduce these terms with high precision

# Results – pole cancellation

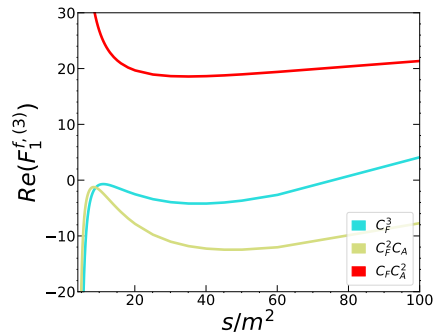
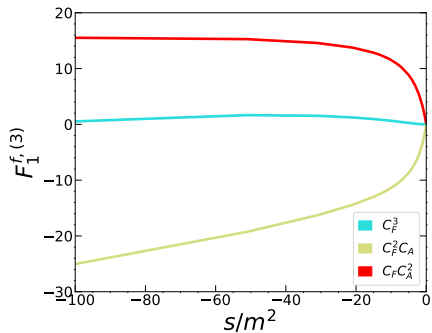
- We use the pole cancellation to estimate the precision
- To estimate the number of significant digits we use

$$\log_{10} \left( \left| \frac{\text{expansion} - \text{analytic CT}}{\text{analytic CT}} \right| \right)$$

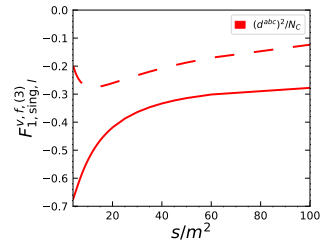
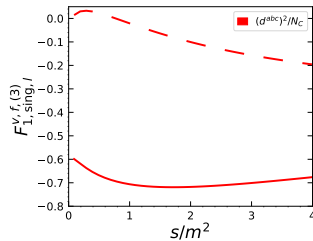
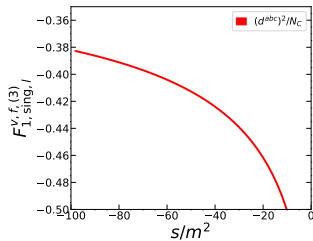
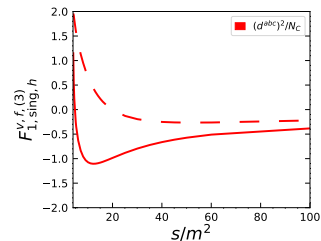
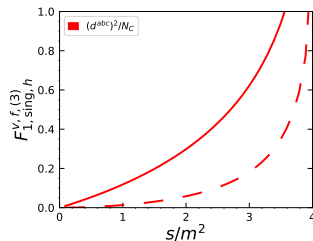
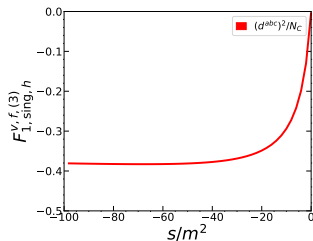
- ⇒ We estimate at least 8 correct digits for the finite terms for QCD and 10 correct digits for QED
- Most regions for most color factors and especially singlet contributions much more precise



# Results – some plots: nonsinglet



# Results – some plots: singlet



## Public implementation – Mathematica

- Bare as well as both ultraviolet and infrared finite form factors implemented as grids for Mathematica:  
formfactors3l

```
Get["FormFactors3l.m"]
```

```
In[] := FormFactorBareNonSing[veF1, 0, -1]
```

```
Out[] := 77.0506 cA^2 cR+95.0634 cA cR^2+0.467466 cR^3
        -21.9243 cA cR I2R nh-11.5582 cR^2 I2R nh+0.751403 cR I2R^2 nh^2
        -62.6063 cA cR I2R nl-45.5408 cR^2 I2R nl+9.35837 cR I2R^2 nh nl
        +11.8102 cR I2R^2 nl^2
```

```
In[] := FormFactorRenNonSing[veF1, -1]
```

```
Out[] := 3.10714 cA^2 cR-3.23413 cA cR^2+0.0144347 cR^3
        +0.0435081 cA cR I2R nh-0.0640418 cR^2 I2R nh
        -0.0107609 cR I2R^2 nh^2-2.59041 cA cR I2R nl
        +1.02032 cR^2 I2R nl+0.000282528 cR I2R^2 nh nl
        +0.494057 cR I2R^2 nl^2
```

## Public implementation – Fortran

- Ultraviolet renormalized, infrared unsubtracted form factors implemented as grids in Fortran library ff3l
- Specialization to QED by adding suffix `_qed` to function calls
- Ready for Monte-Carlo tools

```
program example1
  use ff3l
  implicit none

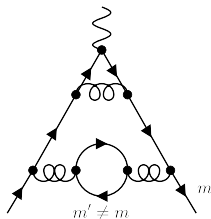
  double complex :: f1v
  double precision :: s = 10
  integer :: eporder

  do eporder = -3,0
    f1v = ff3l_veF1(s,eporder)
    print *, "F1( s = ",s," , ep = ",eporder," ) = ", f1v
  enddo
end program example1
```

# Summary

- Calculated massive form factors at NNNLO in QCD
- Applied a semianalytic method by constructing series expansions and matching numerically
- Reproduce known results from the literature:
  - large- $N_c$  limit,  $n_l$ , and partial  $n_h$  contributions
  - static, high-energy, and threshold expansions
- Checked chiral Ward identity for singlet contributions
- Estimate precision to at least 8 significant digits over the whole real axis for QCD and 10 significant digits for QED
- Results available as grids for both Mathematica and Fortran

# Outlook: contributions with a second mass $m' \neq m$ (extremely preliminary)

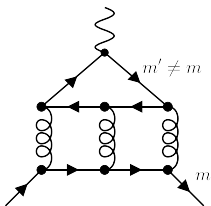


## ■ NNLO:

- 1 bubble diagram
- Can be expressed through dispersion integral over vacuum polarization as for the hadronic corrections [Fael 2018]
- Leptonic vacuum polarization known through four loops in QED [Sturm 2013] and top contribution to three loops in QCD [Chetyrkin, Kühn, Steinhauser 1995 + 1996]

## ■ NNNLO:

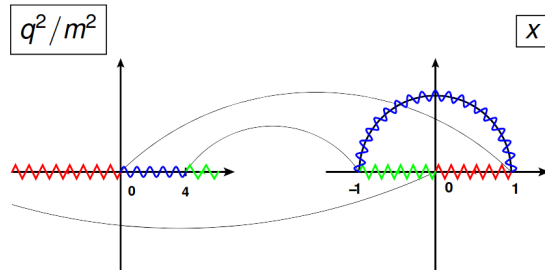
- 42 nonsinglet diagrams, some of them with topologies beyond bubbles
- 152 master integrals
- Boundaries at  $s = 0$  available, but already complicated functions of ratio  $\frac{m'}{m}$  [Fael, Schönwald, Steinhauser 2020]
- Then symbolic expansions in  $\frac{m'}{m}$  and  $\frac{s}{m}$  and match numerically?
- Or solve numerically in relevant range  $\frac{s}{m}$  for fixed  $\frac{m'}{m}$  like [Boughezal, Czakon, Schutzmeier 2007; Czakon, Niggetiedt 2020] ?





# Why numerical?

$$q^2 = s = -\frac{(1-x)^2}{x}$$



- Large- $N_c$  and  $n_h$  contributions at NNNLO can be written as iterated integrals over letters

$$\frac{1}{x}, \frac{1}{1+x}, \frac{1}{1-x}, \frac{1}{1-x+x^2}, \frac{x}{1-x+x^2}$$

- $n_h$  terms already contain structures beyond iterated integrals (elliptic integrals)
- ⇒ No ready-to-use tools available for analytic solution
- ⇒ Instead: Full solution through analytic series expansions and numerical matching

# Series expansions

- Different ansätze for different points:

regular point:

$$M_n(\epsilon, \hat{s} = \hat{s}_0) = \sum_{i=-3}^{\infty} \sum_{j=0}^{j_{\max}} c_{ij}^{(n)} \epsilon^i (\hat{s} - \hat{s}_0)^j$$

# Series expansions

- Different ansätze for different points:

regular point:

$$M_n(\epsilon, \hat{s} = \hat{s}_0) = \sum_{i=-3}^{\infty} \sum_{j=0}^{j_{\max}} c_{ij}^{(n)} \epsilon^i (\hat{s} - \hat{s}_0)^j$$

$s = \pm\infty$  (high-energy limit):

$$M_n(\epsilon, \hat{s} \rightarrow \pm\infty) = \sum_{i=-3}^{\infty} \sum_{j=-s_{\min}}^{j_{\max}} \sum_{k=0}^{i+6} c_{ijk}^{(n)} \epsilon^i \hat{s}^{-j} \ln^k(\hat{s})$$

# Series expansions

- Different ansätze for different points:

regular point: 
$$M_n(\epsilon, \hat{s} = \hat{s}_0) = \sum_{i=-3}^{\infty} \sum_{j=0}^{j_{\max}} c_{ij}^{(n)} \epsilon^i (\hat{s} - \hat{s}_0)^j$$

$s = \pm\infty$  (high-energy limit): 
$$M_n(\epsilon, \hat{s} \rightarrow \pm\infty) = \sum_{i=-3}^{\infty} \sum_{j=-s_{\min}}^{j_{\max}} \sum_{k=0}^{i+6} c_{ijk}^{(n)} \epsilon^i \hat{s}^{-j} \ln^k(\hat{s})$$

$s = 4m^2$  (2-particle threshold): 
$$M_n(\epsilon, \hat{s} = 4) = \sum_{i=-3}^{\infty} \sum_{j=-s_{\min}}^{j_{\max}} \sum_{k=0}^{i+3} c_{ijk}^{(n)} \epsilon^i [\sqrt{4 - \hat{s}}]^j \ln^k(\sqrt{4 - \hat{s}})$$

# Series expansions

- Different ansätze for different points:

regular point: 
$$M_n(\epsilon, \hat{s} = \hat{s}_0) = \sum_{i=-3}^{\infty} \sum_{j=0}^{j_{\max}} c_{ij}^{(n)} \epsilon^i (\hat{s} - \hat{s}_0)^j$$

$s = \pm\infty$  (high-energy limit): 
$$M_n(\epsilon, \hat{s} \rightarrow \pm\infty) = \sum_{i=-3}^{\infty} \sum_{j=-s_{\min}}^{j_{\max}} \sum_{k=0}^{i+6} c_{ijk}^{(n)} \epsilon^i \hat{s}^{-j} \ln^k(\hat{s})$$

$s = 4m^2$  (2-particle threshold): 
$$M_n(\epsilon, \hat{s} = 4) = \sum_{i=-3}^{\infty} \sum_{j=-s_{\min}}^{j_{\max}} \sum_{k=0}^{i+3} c_{ijk}^{(n)} \epsilon^i [\sqrt{4 - \hat{s}}]^j \ln^k(\sqrt{4 - \hat{s}})$$

$s = 16m^2$  (4-particle threshold): 
$$M_n(\epsilon, \hat{s} = 16) = \sum_{i=-3}^{\infty} \sum_{j=-s_{\min}}^{j_{\max}} \sum_{k=0}^{i+3} c_{ijk}^{(n)} \epsilon^i [\sqrt{16 - \hat{s}}]^j \ln^k(\sqrt{16 - \hat{s}})$$

# Series expansions

- Different ansätze for different points:

regular point: 
$$M_n(\epsilon, \hat{s} = \hat{s}_0) = \sum_{i=-3}^{\infty} \sum_{j=0}^{j_{\max}} c_{ij}^{(n)} \epsilon^i (\hat{s} - \hat{s}_0)^j$$

$s = \pm\infty$  (high-energy limit): 
$$M_n(\epsilon, \hat{s} \rightarrow \pm\infty) = \sum_{i=-3}^{\infty} \sum_{j=-s_{\min}}^{j_{\max}} \sum_{k=0}^{i+6} c_{ijk}^{(n)} \epsilon^i \hat{s}^{-j} \ln^k(\hat{s})$$

$s = 4m^2$  (2-particle threshold): 
$$M_n(\epsilon, \hat{s} = 4) = \sum_{i=-3}^{\infty} \sum_{j=-s_{\min}}^{j_{\max}} \sum_{k=0}^{i+3} c_{ijk}^{(n)} \epsilon^i [\sqrt{4 - \hat{s}}]^j \ln^k(\sqrt{4 - \hat{s}})$$

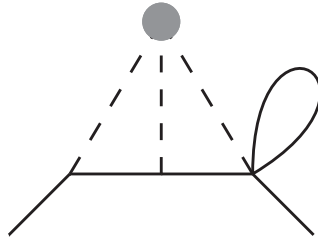
$s = 16m^2$  (4-particle threshold): 
$$M_n(\epsilon, \hat{s} = 16) = \sum_{i=-3}^{\infty} \sum_{j=-s_{\min}}^{j_{\max}} \sum_{k=0}^{i+3} c_{ijk}^{(n)} \epsilon^i [\sqrt{16 - \hat{s}}]^j \ln^k(\sqrt{16 - \hat{s}})$$

- We construct expansions up to  $j_{\max} = 50$  around

$$\hat{s} = \{ -\infty, -32, -28, -24, -16, -12, -8, -4, 0, 1, 2, 5/2, 3, 7/2, 4, 9/2, 5, 6, 7, 8, 10, 12, 14, 15, 16, 17, 19, 22, 28, 40 \}$$

and similar for the  $n_h$ -singlet contributions

# Calculation of boundary conditions – $n_h$ -singlets



- The singlet diagrams can have massless cuts, therefore the limit  $\hat{s} \rightarrow 0$  demands an asymptotic expansion.
  - We reveal regions with ASY.m [Smirnov, Pak 2010; Jantzen, Smirnov, Smirnov 2012] ( $y = \sqrt{-\hat{s}}$ ):
    - ✓  $y^{-0\epsilon}$ : Taylor expansion of the integrand, same as for the non-singlet
    - ✓  $y^{-2\epsilon}$ : integrals can be performed for general  $\epsilon$  in terms of  $\Gamma$  functions
    - ✓  $y^{-4\epsilon}$ : one integral was calculated using HyperInt [Panzer 2014]
- ⇒ We obtain analytic boundary conditions in the limit  $\hat{s} \rightarrow 0$ .

# Calculation of boundary conditions – $n_l$ -singlets

- The singlet diagrams can have massless cuts, therefore the limit  $\hat{s} \rightarrow 0$  demands an asymptotic expansion.
  - We reveal regions with ASY.m [Smirnov, Pak 2010; Jantzen, Smirnov, Smirnov 2012] ( $y = \sqrt{-\hat{s}}$ ):
    - ✓  $y^{-0\epsilon}$ : taylor expansion of the integrand, same as for the non-singlet
    - ✓  $y^{-2\epsilon}$ : integrals can be performed for general  $\epsilon$  in terms of  $\Gamma$  functions
    - ✓  $y^{-4\epsilon}$ : integrals can be performed with HyperInt and Mellin-Barnes methods
    - ✗  $y^{-6\epsilon}$ : direct integration for some integrals quite involved
- ⇒ For the  $n_l$ -singlets we changed strategy and calculated the masters at  $\hat{s} = -1$  with AMFLow [Liu, Ma 2022] and matched from there.



# Moebius Transformations

- The radius of convergence is at most the distance to the closest singularity.
- We can extend the radius of convergence by changing to a new expansion variable.
- If we want to expand around the point  $x_k$  with the closest singularities at  $x_{k-1}$  and  $x_{k+1}$ , we can use:

$$y_k = \frac{(x - x_k)(x_{k+1} - x_{k-1})}{(x - x_{k+1})(x_{k-1} - x_k) + (x - x_{k-1})(x_{k+1} - x_k)}$$

- The variable change maps  $\{x_{k-1}, x_k, x_{k+1}\} \rightarrow \{-1, 0, 1\}$ .

# Renormalization and infrared structure

## UV renormalization

- $\overline{\text{MS}}$  renormalization of  $\alpha_s$
- On-shell renormalization of mass  $Z_m^{\text{OS}}$ , wave function  $Z_2^{\text{OS}}$ , and (if needed) currents [Chetyrkin, Steinhauser 1999; Melnikov, van Ritbergen 2000]
- Much more involved renormalization for the axial and pseudoscalar singlet contributions

## IR subtraction

- Structure of infrared poles given by cusp anomalous dimension  $\Gamma_{\text{cusp}}$  [Grozin, Henn, Korchemski, Marquard 2014]
- Define finite form factors  $F = Z_{\text{IR}} F^{\text{finite}}$  with UV-renormalized form factor  $F$  and

$$Z_{\text{IR}} = 1 - \frac{\alpha_s}{\pi} \frac{1}{2\epsilon} \Gamma_{\text{cusp}}^{(1)} - \left(\frac{\alpha_s}{\pi}\right)^2 \left( \frac{\dots}{\epsilon^2} + \frac{1}{4\epsilon} \Gamma_{\text{cusp}}^{(2)} \right) - \left(\frac{\alpha_s}{\pi}\right)^3 \left( \frac{\dots}{\epsilon^3} + \frac{\dots}{\epsilon^2} + \frac{1}{6\epsilon} \Gamma_{\text{cusp}}^{(3)} \right)$$

- $\Gamma_{\text{cusp}} = \Gamma_{\text{cusp}}(x)$  depends on kinematics
- $\Gamma_{\text{cusp}}$  universal for all currents

## Treatment of $\gamma_5$

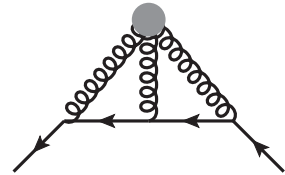
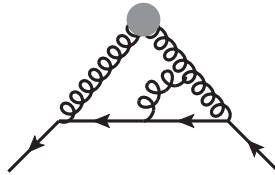
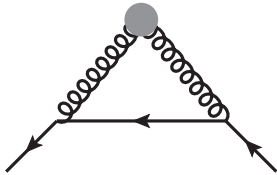
- For non-singlet diagrams always an even number of  $\gamma_5$  matrices appear on a fermion line.  
 ⇒ Use anti-commuting  $\gamma_5$ .
- In the singlet diagrams odd numbers of  $\gamma_5$  appear on a fermion line.  
 ⇒ Use Larin's prescription [Larin 1992]:

$$\gamma_\mu \gamma_5 \rightarrow \frac{1}{3!} \epsilon_{\mu\nu\rho\sigma} \gamma^\nu \gamma^\rho \gamma^\sigma,$$

where the contraction of two  $\epsilon$  tensors is done in  $d = 4 - 2\epsilon$  dimensions.

- ✓ Finite (multiplicative) renormalization constants for all currents are known.
- Only the sum of singlet and non-singlet diagrams renormalizes multiplicative, so the non-singlet has to be calculated in the Larin scheme as well (we use this as a cross-check).

# Chiral Ward identity



- The non-renormalization of the Adler-Bell-Jackiw (ABJ) anomaly implies:

$$\left(\partial^\mu j_\mu^a\right)_R = 2(j^p)_R + \frac{\alpha_s}{4\pi} T_F (G\tilde{G})_R,$$

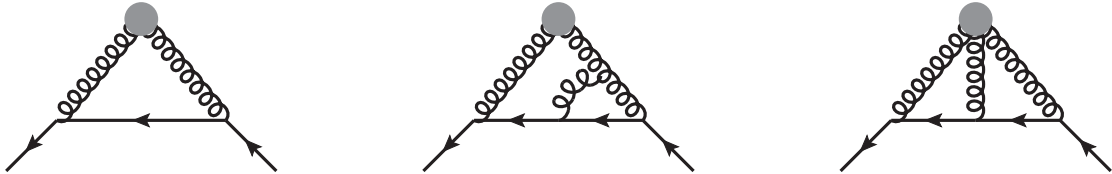
with the pseudoscalar gluonic operator  $G\tilde{G} = \epsilon_{\mu\nu\rho\sigma} G^{a,\mu\nu} G^{a,\rho\sigma}$

- This relation can be used to check the correct treatment of  $\gamma_5$ .
- For the form factors this leads to the identity:

$$F_{\text{sing},1}^{a,f} + \frac{S}{4m^2} F_{\text{sing},2}^{a,f} = F_{\text{sing}}^{p,f} + \frac{\alpha_s}{4\pi} T_F F_{G\tilde{G}}^f$$

- We calculated the form factor associated to  $G\tilde{G}$  up to  $\mathcal{O}(\alpha_s^2)$  for this check.

# Chiral Ward identity



- The new topologies introduce 3 (1), 24 (15) master integrals (new wrt. the form factor calculation).
- We calculate the masters by the algorithm outlined in [\[Ablinger, Blümlein, Marquard, Rana, Schneider 2018\]](#) :
  - ① Uncouple coupled blocks of the differential equation into a higher order one with `0reSys` [\[Gerhold 2002\]](#) and `Sigma` [\[Schneider 2007\]](#) .
  - ② Solve the higher order differential equations via the factorization of the differential operator with `HarmonicSums` [\[Ablinger 2011-\]](#) .
  - ③ The boundary conditions can be found by direct integration in the asymptotic limit  $\hat{s} \rightarrow 0$ .
- We can express the result up to  $\mathcal{O}(\alpha_s^2)$  in terms of harmonic polylogarithms. [\[Remiddi, Vermaseren 1999\]](#)

## Results – threshold expansion around $s = 4m^2$

- Close to threshold we can construct cross-sections and decay rates like

$$\sigma(e^+e^- \rightarrow Q\bar{Q}) = \sigma_0\beta \underbrace{\left( |F_1^v + F_2^v|^2 + \frac{|(1-\beta^2)F_1^v + F_2^v|^2}{2(1-\beta^2)} \right)}_{=3/2 \Delta^v}$$

with the quark velocity  $\beta = \sqrt{1 - 4m^2/s}$

- Real radiation suppressed by  $\beta^3$
- ⇒ Direct phenomenological relevance
- We find (with  $l_{2\beta} = \ln(2\beta)$ )

$$\begin{aligned} \Delta^{v,(3)} = & C_F^3 \left[ -\frac{32.470}{\beta^2} + \frac{1}{\beta} (14.998 - 32.470 l_{2\beta}) \right] + C_A^2 C_F \frac{1}{\beta} [16.586 l_{2\beta}^2 - 22.572 l_{2\beta} + 42.936] \\ & + C_A C_F^2 \left[ \frac{1}{\beta^2} (-29.764 l_{2\beta} - 7.7703) + \frac{1}{\beta} (-12.516 l_{2\beta} - 11.435) \right] \\ & + \mathcal{O}(\beta^0) + \text{fermionic contributions} \end{aligned}$$

- Agrees with dedicated calculation [Kiyoy, Maier, Maierhöfer, Marquard 2009]